



OPEN ACCESS

EDITED BY

Joao Henrique Lopes,
Aeronautics Institute of Technology (ITA), Brazil

REVIEWED BY

Lin Yang,
Helmholtz Association of German Research
Centres (HZ), Germany
Jing Zhao,
Zhejiang University, China

*CORRESPONDENCE

Teja Guda,
✉ teja.guda@utsa.edu

RECEIVED 06 November 2024

ACCEPTED 04 February 2025

PUBLISHED 26 February 2025

CITATION

Gonzales G, Malka R, Bizios R, Dion GR and
Guda T (2025) Burn inhalation injury and
intubation with dexamethasone-eluting
endotracheal tubes modulate local microbiome
and alter airway inflammation.
Front. Bioeng. Biotechnol. 13:1524013.
doi: 10.3389/fbioe.2025.1524013

COPYRIGHT

© 2025 Gonzales, Malka, Bizios, Dion and Guda.
This is an open-access article distributed under
the terms of the [Creative Commons Attribution
License \(CC BY\)](https://creativecommons.org/licenses/by/4.0/). The use, distribution or
reproduction in other forums is permitted,
provided the original author(s) and the
copyright owner(s) are credited and that the
original publication in this journal is cited, in
accordance with accepted academic practice.
No use, distribution or reproduction is
permitted which does not comply with these
terms.

Burn inhalation injury and intubation with dexamethasone-eluting endotracheal tubes modulate local microbiome and alter airway inflammation

Gabriela Gonzales¹, Ronit Malka², Rena Bizios¹, Gregory R. Dion³
and Teja Guda^{1,4*}

¹Department of Biomedical Engineering and Chemical Engineering, University of Texas at San Antonio, San Antonio, TX, United States, ²Department of Otolaryngology – Head and Neck Surgery, Brooke Army Medical Center JBSA Fort Sam Houston, San Antonio, TX, United States, ³Department of Otolaryngology – Head and Neck Surgery, University of Cincinnati, Cincinnati, OH, United States, ⁴Department of Cell Systems and Anatomy, University of Texas Health San Antonio, San Antonio, TX, United States

Background: Inhalation injuries, caused by exposure to extreme heat and chemical irritants, lead to complications with speaking, swallowing, and breathing. This study investigates the effects of thermal injury and endotracheal tube (ETT) placement on the airway microbiome and inflammatory response. A secondary aim is to assess the impact of localized dexamethasone delivery via a drug-eluting ETT to reduce laryngeal scarring.

Methods: Inhalation injury was developed in swine by administering heated air (150°C–160°C) under endoscopic visualization. Following injury, segments of regular or dexamethasone-loaded endotracheal tubes (ETTs) were placed in the injured airways for 3 or 7 days. Computed tomography (CT) scans were used to assess airway narrowing post-injury. Biofilm formation on the ETTs was investigated using micro-CT and microscopy. The airway microbiome was analyzed via 16S rRNA sequencing. Inflammatory markers were quantified using an immunoassay and macrophage populations in laryngeal tissue were assessed with CD86 and CD206 staining. Tracheal tissues were also histologically examined for epithelial thickness, collagen area, and mucin production.

Results: CT scans confirmed airway narrowing post-injury, particularly around ETT sites. Biofilm formation was more extensive on dexamethasone-coated ETTs at later timepoints. Beta diversity analysis revealed significant shifts in microbial composition related to ETT type ($R^2 = 0.04$, $p < 0.05$) and duration of placement ($R^2 = 0.22$, $p < 0.05$). Differential abundance analysis demonstrated significant positive log fold changes in genera such as *Bergeriella*, *Peptostreptococcus*, and *Bacteriodes* with thermal injury over time. Inflammatory markers IFN- γ , IL-4, and IL-1 β were elevated in dexamethasone-ETT groups at 3 days, then decreased by 7 days. Macrophage markers CD86 and CD206 were significantly greater in dexamethasone groups compared to regular ETT groups at 7 days ($p = 0.002$ and

$p = 0.0213$, respectively). Epithelial thickness was significantly greater with regular ETT placement compared to dexamethasone ETT placement in the burn-injured airway at 3 days ($p = 0.027$).

Conclusion: Thermal inhalation injury and ETT placement significantly impact airway inflammation, structural integrity, and microbiome composition. Dexamethasone-eluting ETTs, intended to reduce inflammation, increased biofilm formation and elevated cytokine levels, suggesting complex interactions between the drug coating and the host immune response. The airway microbiome shifted significantly with specific taxa thriving in the inflamed environment.

KEYWORDS

inhalation injury, upper airway, microbiome, inflammation, endotracheal tube

Introduction

Severe burn injuries are often accompanied by inhalation injuries, involving acute damage to the respiratory system caused by exposure to chemicals and/or heat (Monteiro et al., 2017; Charles et al., 2022). This occurs because of the glottic closure reflex—the instinctive adduction of the vocal folds protecting the lower airways causing the vocal folds themselves to brace the impact of heat exposure. Additionally, insult below the glottis can result from the irritants present in smoke. Such injuries can lead to delayed airway edema often necessitating ventilatory support and generally requiring prophylactic intubation (Foncerrada et al., 2018; Cochran, 2009; Orozco-Peláez, 2018). Acute tissue injury and subsequent use of indwelling medical devices, such as endotracheal tubes (ETTs), disrupts the respiratory mucosal barrier, increasing the risk of infections like pneumonia (Ronkar et al., 2023; Edelman et al., 2007). More severe complications that can arise include acute respiratory distress syndrome (ARDS), or stenosis due to the accumulation of laryngeal or tracheal scar tissue (Bittner and Sheridan, 2023; Jones et al., 2017; Gaissert et al., 1993).

The microbiome of the respiratory tract plays an integral role in maintaining immune homeostasis and influencing disease pathology. Trauma, such as inhalation injury, can lead to dysbiosis between microbes which often results in favor of opportunistic pathogenic microbes (Natalini et al., 2023). Bacterial infections, often the precursor to pneumonia, are frequently identified through histological examination and culturing respiratory mucous secretions (Torres et al., 2016). However, these methods can miss rare or less abundant taxa that can play significant roles in the development of chronic diseases. To address these limitations, 16S rRNA sequencing has emerged as a valuable technique for providing a comprehensive view of the bacterial species present. This method has been extensively used to study bacteria associated with inflammatory airway diseases such as chronic obstructive pulmonary disease (COPD) and asthma, revealing taxa that thrive in inflamed microenvironments (Ramsheh et al., 2021; Wang et al., 2016; Leiten et al., 2020; Millares et al., 2015; Pragman et al., 2012; Tangedal et al., 2019; Marri et al., 2013; Morimoto et al., 2024). Despite these advances, our current knowledge of the airway microbiome's precise role in inhalation injury sequelae remains limited, indicating a significant gap that requires further investigation (Dyamenahalli et al., 2019).

In parallel, airway inflammation is a natural response to injury and a part of the healing process. Following damage, immune cells

are recruited to the site of injury to remove pathogens and initiate tissue repair (Aghasafari et al., 2019; Huber-Lang et al., 2018). This acute inflammatory response is characterized by the release of various cytokines and chemokines that help to regulate the body's defenses but, if persistent, can exacerbate the injury and delay healing. Chronic inflammation is often associated with an imbalance between pro-inflammatory and anti-inflammatory mediators such as different macrophage phenotypes (Chang-Hoon and Eun Young, 2018; Koh and DiPietro, 2011). Understanding the mechanisms underlying immune response in inhalational injury can contribute towards the development of effective treatments for these conditions, potentially preventing long-term complications.

Airway mucins are major components of mucus, a gel-like substance that lines the mucosal epithelium and protects the airway from inhaled pathogens and toxins (Song et al., 2020). Mucus facilitates the expulsion of irritants through mucociliary clearance or coughing. In healthy individuals, mucus production is continuous, maintaining a balanced and protective layer (Pangeni et al., 2023). Biofilms, however, are structured communities of microorganisms encased in a self-produced extracellular matrix (Hall-Stoodley and McCoy, 2022; Domingue et al., 2020). They often adhere to surfaces such as endotracheal tubes and can stimulate the production of additional mucins, potentially leading to hypersecretion (Mishra et al., 2024; Powell et al., 2018). Both excessive mucus and biofilm presence can exacerbate inflammatory responses, as they create a favorable environment for sustained immune activation and persistent microbial colonization (Moser et al., 2017; Fahy and Dickey, 2010). Inhalation injuries can cause pathophysiologic changes, including thickened mucus, loss of surfactant, and impaired mucociliary function (Foncerrada et al., 2018; Cox et al., 2008). Exploring the alterations in mucus secretion and ETT biofilm formation associated with thermal inhalation injury could thus provide valuable insights into the inflammatory response to design timely interventions and corticosteroid or other interventional therapy leading to potential improvements in patient outcomes and quality of care.

The objective of this study was to investigate the effects of thermal inhalation injury and ETT placement on the interdependency between the microbiome and inflammatory response in the upper airway. A secondary objective was to evaluate the impact of localized delivery of dexamethasone on these outcomes using a drug-eluting ETT to prevent excessive laryngeal scarring and stenosis.

Materials and methods

Study design

The current study was approved by the U.S. Air Force 59th Medical Wing Institutional Animal Care and Use Committee (protocol FWH20210102AR). An experimental overview is presented in Figure 1. Laryngeal thermal injury was simulated in Yorkshire crossbred swine under endoscopic visualization. Endotracheal tube (ETT) segments, with or without a dexamethasone-eluting electrospun fiber coating, were then placed for either 3 days ($n = 5$) or 7 days ($n = 4$). Biofilm formation and bacterial adhesion were examined using scanning electron microscopy (SEM), micro-computed tomography (μ CT), and histology. Changes in the microbiome following injury and ETT placement were assessed through 16S rRNA sequencing. The inflammatory response of the upper airway was evaluated using immunohistochemistry and immunoassays. Additionally, histological evaluation of the trachea was conducted to assess epithelial changes.

Endotracheal tube coating

ETTs were coated via electrospinning as previously described by our group (Gonzales et al., 2024). Briefly, polycaprolactone (PCL)

(Mw = 80,000) was dissolved in chloroform (15:85 w/w) and dexamethasone sodium phosphate was added to the homogeneous mixture at a concentration of 10% (PCL:Drug) along with its solvent ethanol.

The solution was then loaded into a Luer Lock syringe and dispensed through an 18G blunt tip needle using a syringe pump (Pump11 Elite, Harvard Apparatus, Holliston, MA) at a rate of 1.8 mL/hr. A 5 cm section of section of an ETT (7-0, Aircare[®]) was positioned on a rotating rod (300 rpm) 20 cm below the needle tip where a voltage of 20 kV was applied (Gamma High Voltage Research, Ormond Beach, FL). The coated ETTs were subsequently sterilized with ethylene oxide before use. Using only a section of the ETT was intended to enable the animals to maintain normal activity throughout the study instead of being sedated and intubated for extended periods. Unless otherwise specified, chemicals were sourced from Sigma-Aldrich (St. Louis, MO).

Laryngeal inhalation injury simulation and ETT placement

Animals were anesthetized with intramuscular Telazol[®] and Ketamine (2.2 mg/kg) and maintained on 0.5%–5% isoflurane during the procedure. Pain relief was provided with intramuscular Buprenorphine (0.01–0.05 mg/kg). Laryngeal burn

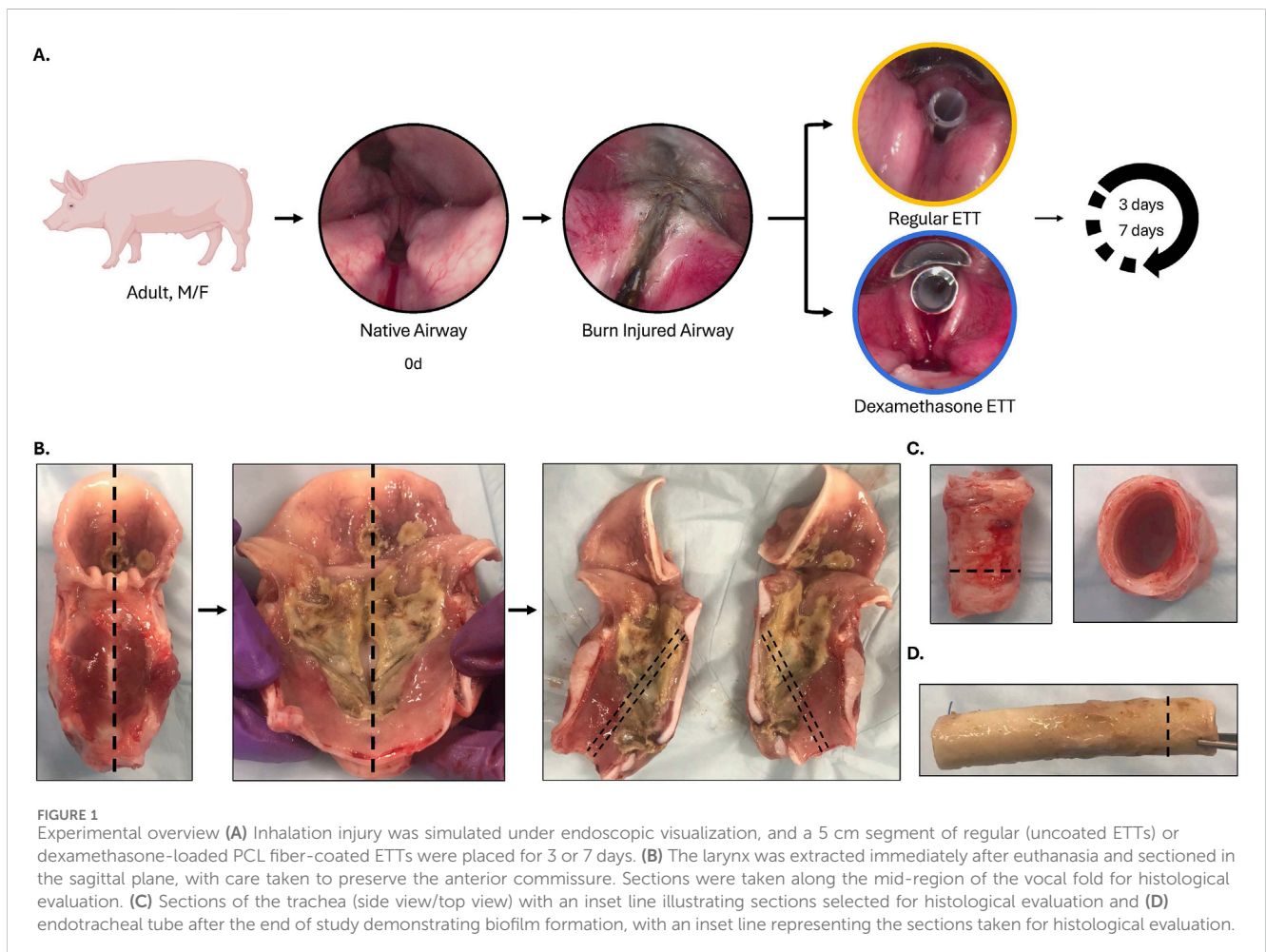


FIGURE 1 Experimental overview (A) Inhalation injury was simulated under endoscopic visualization, and a 5 cm segment of regular (uncoated ETTs) or dexamethasone-loaded PCL fiber-coated ETTs were placed for 3 or 7 days. (B) The larynx was extracted immediately after euthanasia and sectioned in the sagittal plane, with care taken to preserve the anterior commissure. Sections were taken along the mid-region of the vocal fold for histological evaluation. (C) Sections of the trachea (side view/top view) with an inset line illustrating sections selected for histological evaluation and (D) endotracheal tube after the end of study demonstrating biofilm formation, with an inset line representing the sections taken for histological evaluation.

injuries were created as previously described (Malka et al., 2023) by administering heated air (150°C–160°C) to the larynx of spontaneously breathing animals in 30-s intervals for 5 min at a rate of 5–10 mL/min under endoscopic visualization.

During direct laryngoscopy, a second surgeon assisted with ETT segment placement. The neck area was prepped with povidone-iodine solution, and 1% lidocaine with epinephrine was injected at the level of the cricoid cartilage. A 3–4 cm midline neck incision was made, and dissection was performed to expose the first three to four tracheal rings. Two 16-gauge angiocatheter needles were inserted into the larynx, one through the cricothyroid membrane and the other between the first and second tracheal rings. A urologic snare was passed through each angiocatheter and out through the mouth. The surgeon passed a 2–0 polypropylene suture through the distal end of the ETT segment, securing each end of the suture to the snares, which were then retracted back through the angiocatheters and the neck. The sutures were pulled taut while the ETT segment was positioned in the larynx, with the lower edge in the subglottis and the upper edge just past the epiglottis. Postoperatively, each animal was monitored hourly for the first 4 h, every 4 h for the next 20 h, and at least twice daily until the end of the study to ensure proper respiratory status.

Euthanasia was carried out with intravenous pentobarbital (100 mg/kg) and confirmed by monitoring vital signs according to institutional protocols. Animals experiencing distress or illness were euthanized earlier than the scheduled postoperative date. The larynx was extracted immediately post-euthanasia, sectioned in the sagittal plane, and frozen at –80°C for subsequent analysis.

Large animal computed tomography

Immediately after the placement of ETTs, animals underwent a computed tomography (CT) scan (Toshiba America Medical Systems Inc., Tustin, CA) with 0.625 mm slice thickness and images were saved in digital imaging and communications in medicine (DICOM) format (Carlisle et al., 2019). Raw images were input into Mimics (Materialise NV, Leuven, Belgium) and the airway region where the ETT was placed was reconstructed into a 3D model. Briefly, a new mask was created based on a “custom” range of Hounsfield Unit (HU) values from –650 to –200 to highlight the airway tissue. From this airway mask, a 3D part was reconstructed and the surface area (SA, mm²) and volume (V, mm³) of the part were obtained. The SA/V ratio was then measured as an imaging biomarker for luminal narrowing.

Biofilm quantification

Following euthanasia, the extracted ETTs were placed in 10% formalin. The samples were stained with phosphotungstic acid (PTA) and imaged with micro computed tomography (μ CT) (Skyscan 1,076, Bruker, Billerica, MA). The ETT scans were imported into Mimics (Materialise NV, Leuven, Belgium) where the tube, biofilm, and guide wire were spatially distinguished. The volume, area, and surface area of the biofilm inclusions were determined from the segmented 3D models. Following μ CT

scanning, a section (~1 cm) of the ETT was set aside for histological analysis and SEM.

Gram staining of ETT

ETT sections were embedded in optimal cutting temperature compound (Scigen Tissue Plus O.C.T. Compound, Thermo Fisher Scientific, Waltham, MA) and stored at –80°C. Samples were sectioned with a cryostat (Eprexia™ NX70, Kalamazoo, MI) to a thickness of 20 μ m, thaw-mounted onto glass slides, and Gram stained (Harleco Gram Stain Set, Sigma-Aldrich, St. Louis, MO). The prepared slide was flooded with crystal violet solution (1 min) and gently rinsed with distilled water. The slides were then flooded with gram iodine solution (1 min) and rinsed gently with distilled water. The samples were decolorized until the solution ran colorless from the slide and washed with distilled water. Finally, the slide was flooded with safranin stain (1 min), rinsed gently with distilled water, and mounted with permount mounting medium (ThermoFisher Scientific, Waltham, MA).

ETT surface characterization

SEM was used to evaluate the morphology of the ETT surfaces after placement. All specimens were dried using a critical point drier (Leica, Wetzlar, Germany), sputter coated with silver-palladium (Cressington Scientific Instruments, Watford, United Kingdom), and imaged under 2 kV applied voltage at 1,000x magnification using a Zeiss Crossbeam 340 Focused Ion Beam (FIB)-SEM (ZEISS, Oberkochen, Germany).

16S rRNA sequencing

At each laryngoscopy (initial and end of study), a swab of the larynx/trachea was collected and stored at –80°C. In addition, the surface of the ETT was swabbed following their removal. The samples were given to the UTSA Genomics Core Facility to be amplified and sequenced. In short, a ZymoBIOMICS™ DNA Miniprep kit (Zymo Research) was used to extract bacterial DNA from the samples according to the manufacturer's instructions. Following bacterial DNA isolation, the V3-V4 region of the 16S rRNA gene was amplified using universal primer sets 341F and 805R. Sequences were obtained on an Illumina MiSeq platform (Illumina, San Diego, CA) in a 2 × 300 bp paired-end run using a MiSeq v3 kit and following the 16S Metagenomic Sequencing Library Preparation protocol.

The raw sequencing reads were processed using R Studio (v2021.9.1.372, <http://www.rstudio.com/>). Cutadapt (v4.1) was used for removal of primers from the reads and the DADA2 pipeline (v1.16) was used for subsequent processing (Callahan et al., 2016; Martin, 2011). Briefly, the demultiplexed fastq files for each sample were filtered and trimmed to remove low-quality sequences and run through DADA2's core denoising algorithm to determine inferred composition of the samples. The forward and reverse reads were merged, an amplicon sequence variant (ASV) table was constructed, and chimeras were

removed. Species-level taxonomy was assigned to the sequence variants using the Silva (v138.1) database (Quast et al., 2013). The R packages phyloseq, vegan, and ggplot2 were used for downstream analysis and visualization of the sequencing data (McMurdie and Holmes, 2013).

Immunohistochemistry

Laryngeal tissues were sectioned into a 5 mm thick section along the mid-region of the vocal fold, fixed in 4% formalin overnight, and mounted in disposable embedding molds with O.C.T. Tissue samples were stored at -80°C prior to sectioning with a cryostat to a thickness of $14\ \mu\text{m}$ and thaw-mounting onto glass slides. Slides were thawed at room temperature for 10 min and washed in sterile PBS to rehydrate (2 times, 10 min). They were then permeabilized in 1% goat serum and 0.4% TritonX100 in PBS (2 times, 10 min). Sections were blocked with 5% goat serum in PBS for 1 h at room temperature and placed to air dry for 5 min. Tissue sections were incubated in antibodies anti-CD86 (1:100, ab269587, Abcam, Cambridge, MA) and anti-CD206 (1:50, ab8918, Abcam, Cambridge, MA) in 5% goat serum for 2 h at room temperature. Following incubation, sections were washed with PBS (3 times, 5 min) and incubated in a secondary antibodies Alexa 647 (1:1,000, Cat. A21244, ThermoFisher Scientific, Waltham, MA) and Alexa 546 (1:1,000, Cat. A110033, ThermoFisher Scientific, Waltham, MA) for 1 h at room temperature. Slides were washed in PBS (3 times, 5 min), counterstained with DAPI (Cat. R37606, Invitrogen, Waltham, MA), washed again, and mounted with Prolong Diamond Antifade Mountant (Cat. P36970, Invitrogen, Waltham, MA). The stained slides were imaged using an Operetta CLS (PerkinElmer, Ausin, TX) with a water immersion objective lens, in non-confocal mode at $\times 20$ magnification. Images were analyzed using Harmony 4.9 PhenoLOGIC software (PerkinElmer). First, the nuclei were identified to determine the approximate number of cells. Then, the intensity properties for Alexa 647 and Alexa 546 were used to quantify the number of CD86⁺ and CD206⁺ cells and reported as a percentage of number of positive cells per total number of cells. 4 regions from the epithelium and 4 regions from the vocalis muscle were analyzed for each sample.

Cytokine and chemokine immunoassay

The presence of IFN- α , IFN- γ , IL-1 β , IL-10, IL-12/IL-23p40, IL-4, IL-6, IL-8 (CXCL8), and TNF- α were determined using a ProcartaPlex™ Porcine Panel (Cat. EPX090-60829-901, Invitrogen, Waltham, MA) according to the manufacturer's protocol. Biopsy punches of the trachea were taken and 500 μL of cell lysis buffer (CellLytic™ MT, Sigma Aldrich, St. Louis, MO) was added per 100 mg of tissue along with 10 μL protease inhibitor (ThermoFisher Scientific, Waltham, MA) per 1 mL of lysis reagent. The tissue was homogenized and centrifuged at $14,000 \times g$ for 15 min at 4°C . For tissue homogenates, 25 μL of Universal Assay Buffer was added to 25 μL of the sample to each well. The concentration was measured by running the samples on a Bio-Plex® 200 system using Bio-Plex manager software (Bio-Rad, Hercules, CA).

Histological analysis

Frozen tracheas and mounted in disposable embedding molds with O.C.T. Tissue samples were sectioned with a cryostat to a thickness of $14\ \mu\text{m}$ and thaw-mounted onto glass slides. Slides were stained with hematoxylin and eosin (H&E) (Richard-Allan Scientific™ Signature Series™ Stains, Thermo Fisher Scientific, Waltham, MA), Masson's trichrome (Newcomer Supply, Middleton, WI), and Alcian Blue/Periodic Acid Schiff (Newcomer Supply, Middleton, WI) according to the manufacturer's protocol. A Motic EasyScan Pro 6 Slide Scanner (Motic Instruments, Schertz, TX) was used to image slides at 40X.

Epithelial thickness along the trachea was measured from Masson's trichrome stained samples using ImageJ (Version 1.53k, National Institute of Health, United States). The area of collagen, expressed as percentage of the total area, also based on Masson's trichrome was determined in ImageJ. Briefly, images were deconvoluted using the color deconvolution2 plugin and the percentage of pixels above the threshold (0–105, min-max) in the area above the tracheal cartilage was evaluated using the blue component representative of collagen (Landini et al., 2021). The color deconvolution2 plugin was also used to determine percentage of positive staining for Alcian Blue and Periodic Acid Schiff. Results were reported as a ratio of Alcian Blue to Periodic Acid Schiff (AB: PAS).

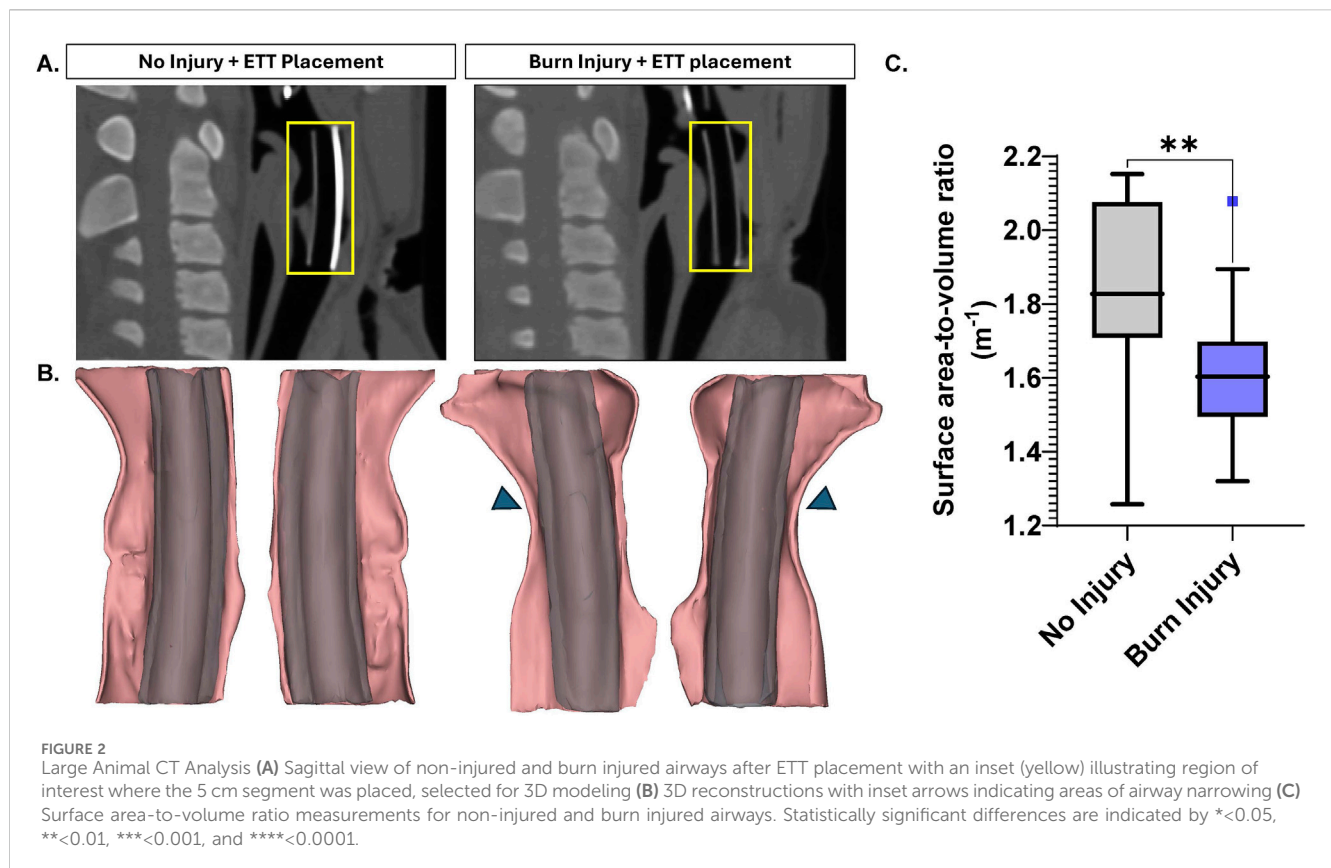
Statistical analysis

Comparison of SA/V ratio between non-injured and burn injured airways with ETT placement was analyzed with an unpaired t-test. For comparing ETT biofilm volume, alpha diversity, macrophage markers, cytokine levels and histological outcomes across ETT type and duration of placement, statistical analysis was performed using a two-way ANOVA followed by Tukey's post hoc test. Alpha diversity was evaluated with Shannon and Chao1 indices to estimate within-sample evenness and richness. The beta diversity describing diversity across samples was assessed with principal coordinate analysis (PCoA) based on the Bray-Curtis dissimilarity index. Statistical differences among groups were determined by permutational analysis of variance (PERMANOVA) using the function adonis from the vegan R package. Differential abundance analysis was performed with ANCOM-BC2 (Lin and Peddada, 2020; Lin et al., 2022) between the regular ETT groups versus dexamethasone ETT groups and 0 days swabs versus swabs taken at 3 and 7 days following the end of study. Significant differences were determined at $p < 0.05$ for all statistical measures.

Results

Surface area-to-volume ratio

Figure 2A presents a sagittal view of the airway following ETT placement in both uninjured and burn injured airways. The 3D renderings of the regions where the ETT sections were placed demonstrated airway narrowing due to burn injury (Figure 2B). Statistically, these differences were significant, with the SA/V ratio being significantly greater in the uninjured airway ($1.84 \pm 0.06\ \text{m}^{-1}$)



compared to the burn injured airway ($1.61 \pm 0.05 \text{ m}^{-1}$, $p = 0.003$) (Figure 2C).

Endotracheal tube biofilm inclusions

Analysis of 3D models based on μ CT data revealed a trend of higher biofilm inclusions in dexamethasone coated ETTs compared to regular ETTs, though the difference did not reach statistical significance (Figure 3). Both ETT types demonstrated a trend of increase in biofilm from 3 days to 7 days. For regular ETTs, the biofilm volume increased from $39.5 \pm 10.8 \text{ mm}^3$ at 3 days to $91.3 \pm 20.4 \text{ mm}^3$ at 7 days. Similarly, dexamethasone coated ETTs exhibited an increase from $124.4 \pm 25.5 \text{ mm}^3$ at 3 days to $211.5 \pm 90.5 \text{ mm}^3$ at 7 days. The coated ETTs had a greater biofilm volume compared to regular ETTs, although differences were not statistically significant ($p = 0.054$). Gram stained ETT sections (Figures 3C, D) demonstrated dense clusters of bacteria, particularly surrounding the tube's circumference. Additionally, Gram staining of the coated ETTs revealed bacteria embedded throughout the coating. SEM further confirmed biofilm formation and an abundant bacterial presence on the surface of both ETT types (Figure 4).

Airway microbiome in the burn injured airway

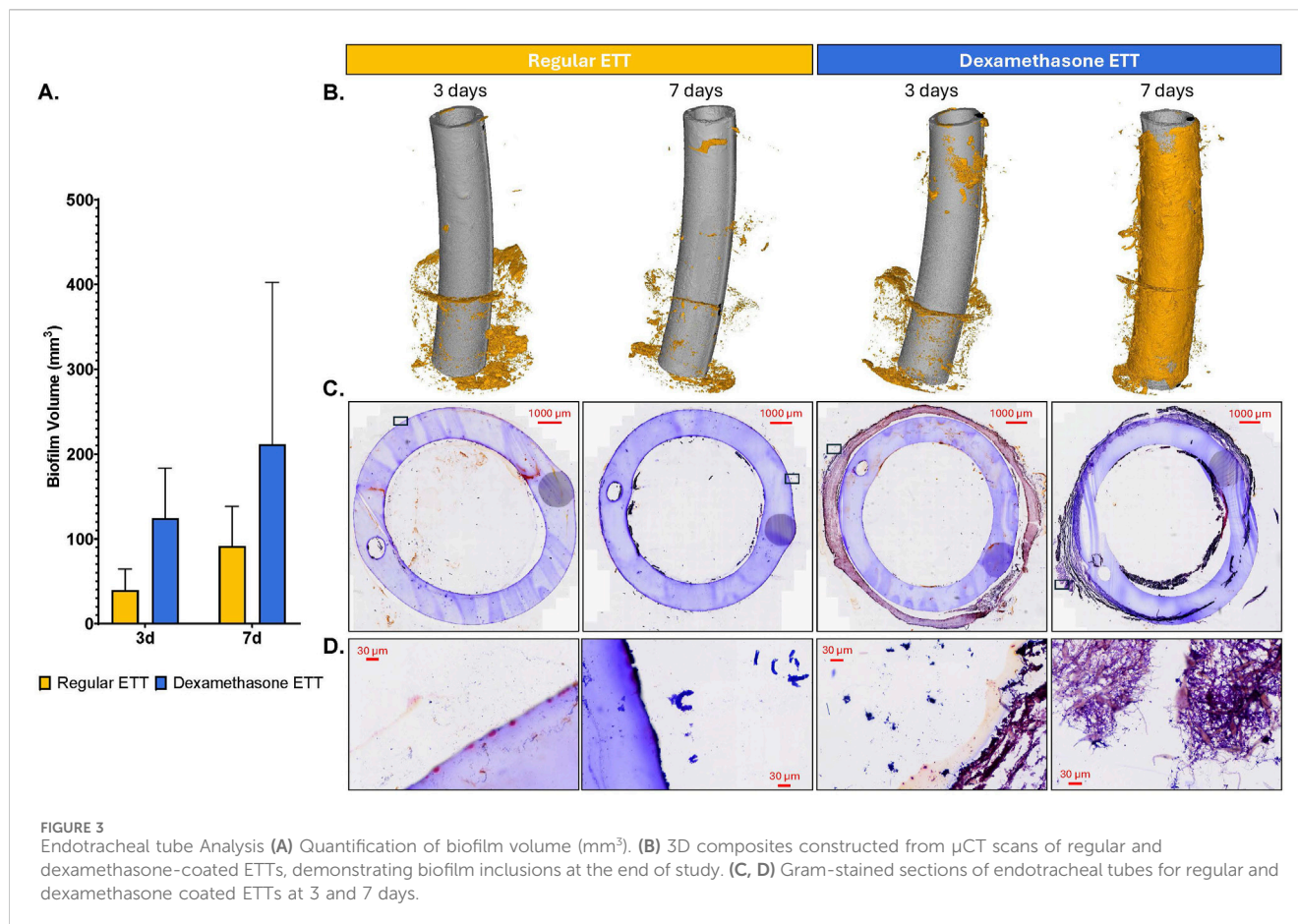
Sequencing of the V3-V4 region of the 16S rRNA gene yielded an average of 75,497 reads per sample. Post-processing with the

DADA2 pipeline resulted in 929,494 reads and identified 7,704 unique sequence variants. In total, 24 phyla, 39 classes, 86 orders, 143 families, and 345 genera were recognized.

Alpha diversity metrics, which measure within-sample species richness and evenness, were evaluated using the Chao1 and Shannon indices (Figure 5A). No significant differences in alpha diversity were observed between ETT types and duration of placement. The top 5 most abundant phyla in across samples were Firmicutes (39.2%), Proteobacteria (25.4%), Bacteroidota (18.8%), Fusobacteriota (10.5%), and Actinobacteriota (5.13%). At the genus level, the predominant genera were *Streptococcus* (14.2%), *Actinobacillus* (12.7%), *Porphyromonas* (11.8%), *Peptostreptococcus* (10.3%), and *Fusobacterium* (9.6%).

The PCoA based on Bray-Curtis dissimilarity accounted for 33.5% of the total variance between samples. Visualization of the plot (Figure 5B) illustrates differences in microbial composition across time points and between ETT types. These differences were statistically confirmed by the PERMANOVA test, which indicated significant variations in the microbial composition related to ETT type ($R^2 = 0.04$, $p < 0.05$) and duration of placement ($R^2 = 0.22$, $p < 0.05$).

Differential abundance analysis revealed no statistically significant differences between ETT types. However, significant changes were observed in several genera over time, as shown in Figure 5C. At 3 days, there were positive log fold changes in *Tyzzellerella* (adj. $p = 0.042$) and *Prevotella_7* (adj. $p = 0.042$), and negative log fold changes in *Staphylococcus* (adj. $p = 0.033$). Additionally, positive log fold changes were observed in *Filifactor* (adj. $p = 0.0007$), *Peptococcus* (adj. $p = 0.001$), and *Fusobacterium*



(adj. $p = 0.008$), while negative log fold changes were seen in *Streptococcus* (adj. $p = 0.002$), *Terrisporobacter* (adj. $p = 0.011$), *Actinobacillus* (adj. $p = 0.002$), and *Rothia* (adj. $p = 0.002$), among others at 7 days. Notably, *Bergeriella* (adj. $p = 0.011$ and adj. $p < 0.0001$, 3 and 7 days, respectively), *Bacteroides* (adj. $p = 0.009$ and adj. $p = 0.009$, 3 and 7 days, respectively), and *Peptostreptococcus* (adj. $p = 0.049$ and adj. $p = 0.019$, 3 and 7 days, respectively) exhibited positive log fold changes at both 3 and 7 days, with these changes increasing from early to late time points. Other significant taxa with detailed p -values are provided in [Supplementary Table S1](#).

Cytokine responses to regular and dexamethasone ETTs in the burn-injured airway

Figure 6 illustrates the evaluation of inflammatory cytokines and chemokines. Tracheal levels of IL-10, TNF- α , IFN- α , and IL-8 did not show any significant differences between ETT types or durations of placement. However, IFN- γ , IL-4, and IL-1 β levels were significantly higher in the dexamethasone ETT groups compared to the regular ETT groups at 3 days ($p = 0.015$, $p = 0.025$, and $p = 0.018$, respectively). IFN- γ levels in the dexamethasone ETT groups significantly decreased from 2.39 ± 0.507 pg/mg protein at 3 days to 0.898 ± 0.081 pg/mg protein at 7 days ($p = 0.032$). Similarly, IL-4 levels significantly decreased from 0.731 ± 0.144 pg/mg protein at 3 days to 0.293 ± 0.034 pg/mg protein at 7 days ($p = 0.039$).

When comparing cytokine levels to control tracheal tissue without burn injury or ETT placement, IL-1 β levels were significantly greater in the dexamethasone ETT groups at 3 days (57.8 ± 5.60 pg/mg protein) and 7 days (35.3 ± 8.90 pg/mg protein) in comparison to the control group (7.70 ± 3.42 pg/mg protein, $p < 0.0001$ and $p = 0.028$, respectively). Similarly, IL-12 levels were significantly higher in the dexamethasone ETT groups at 3 days (30.6 ± 7.84 pg/mg protein) compared to the control group (7.86 ± 3.40 pg/mg protein, $p = 0.015$). IL-6 levels were significantly higher in the regular ETT groups at 3 days (65.0 ± 11.0 pg/mg protein) compared to the control group (1.53 ± 0.340 pg/mg protein, $p = 0.016$).

Macrophage marker expression in burn-injured vocal fold epithelium and vocalis muscle

We analyzed the presence of CD86 and CD206 positive cells, markers for M1 and M2 macrophages respectively (**Figure 7**). In the vocal fold epithelium, CD86 levels increased significantly in the dexamethasone ETT groups from $12.4\% \pm 1.35\%$ at 3 days to $26.6\% \pm 2.99\%$ at 7 days ($p = 0.0004$). Similarly, CD206 levels in the epithelium showed a significant increase in the dexamethasone groups from $14.0\% \pm 1.23\%$ at 3 days to $24.7\% \pm 2.97\%$ at 7 days ($p = 0.0248$). At 7 days, groups with dexamethasone ETT placement had significantly higher percentages of CD86 and CD206 in the

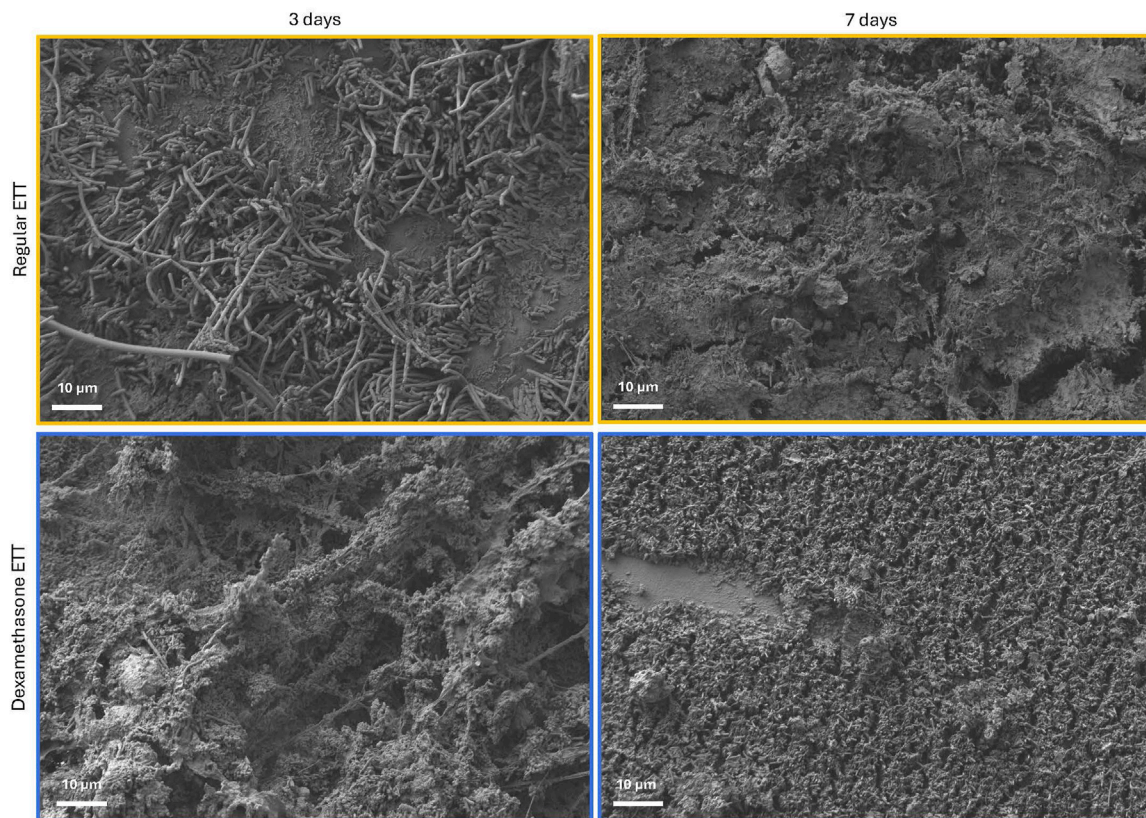


FIGURE 4
SEM micrographs of the surface of regular and dexamethasone-coated ETTs at 3 and 7 days, demonstrating biofilm formation and abundance of bacterial adhesion.

epithelium compared to groups with regular ETT placement ($p = 0.002$ and $p = 0.0213$, respectively). In the vocalis muscle, there was a statistically significant interaction effect between ETT type (regular ETT at 3 days, regular ETT at 7 days, dexamethasone ETT at 3 days, and dexamethasone ETT at 7 days) and macrophage markers (CD86 and CD206) ($p = 0.0053$). This interaction indicates that the impact of ETT type on macrophage marker levels differs depending on the specific marker being analyzed.

Histological analysis of epithelial thickness, percentage area of collagen, and mucins

Histological evaluation of the tracheal epithelium indicated distinct morphological changes with both injury and dexamethasone treatment (Figure 8A). Epithelial thickness (Figure 8B) was significantly greater in tracheal tissue with burn injury and regular ETT placement at both 3 and 7 days ($p = 0.0002$ and $p = 0.0167$, respectively), and with dexamethasone ETT placement at 3 days ($p = 0.004$), compared to healthy control tissue ($32.5 \pm 2.44 \mu\text{m}$). In the regular ETT groups, thickness decreased significantly from $85.5 \pm 7.29 \mu\text{m}$ at 3 days to $69.7 \pm 8.11 \mu\text{m}$ at 7 days ($p = 0.0035$). There was also a significant decrease in epithelial thickness in dexamethasone ETT groups from $73.9 \pm 2.31 \mu\text{m}$ at 3 days to $57.7 \pm 5.85 \mu\text{m}$ at 7 days ($p = 0.0019$). Additionally, epithelial thickness was significantly greater with

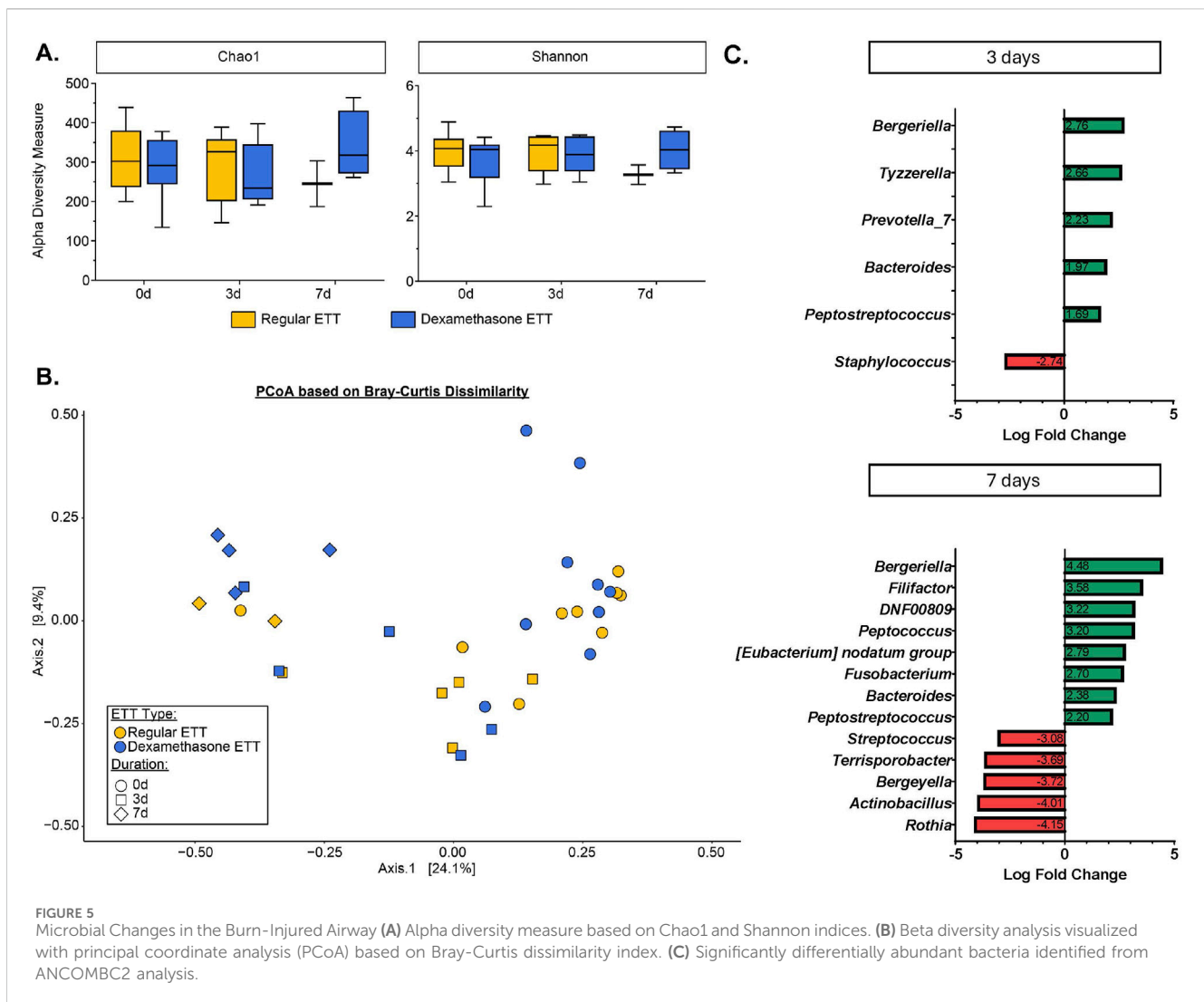
regular ETT placement compared to dexamethasone ETT placement in the burn injured airway at 3 days ($p = 0.027$).

The percentage area of collagen (Figure 8C) remained consistent in the regular ETT groups, measuring $42.5\% \pm 3.33\%$ at 3 days and $42.5\% \pm 4.37\%$ at 7 days. Similarly, in the dexamethasone ETT groups, collagen area was $42.1\% \pm 3.06\%$ at 3 days and $42.7\% \pm 3.11\%$ at 7 days. These values were lower than the percentage area of collagen detected in the control tracheal tissue without injury or ETT placement ($50.9\% \pm 5.61\%$), however, the differences were not statistically significant.

Alcian Blue: Periodic Acid Schiff (AB/PAS) percentage ratios (Figure 8D) were also measured to distinguish changes in acidic and neutral mucins in the tracheal tissue above the hyaline cartilage. In the regular ETT groups, AB/PAS ratio decreased from 3.62 ± 0.38 at 3 days to 1.88 ± 0.14 at 7 days. In contrast, in the dexamethasone ETT groups, the AB/PAS ratio increased from 3.56 ± 0.67 at 3 days to 8.37 ± 3.32 at 7 days. These values were higher than control trachea without burn injury or ETT placement (0.92 ± 0.32), although differences were not statistically significant.

Discussion

Inhalation injury, resulting from inhaling extreme heat or chemicals, is a significant factor contributing to increased mortality in burn victims (Monteiro et al., 2017; Smith et al.,

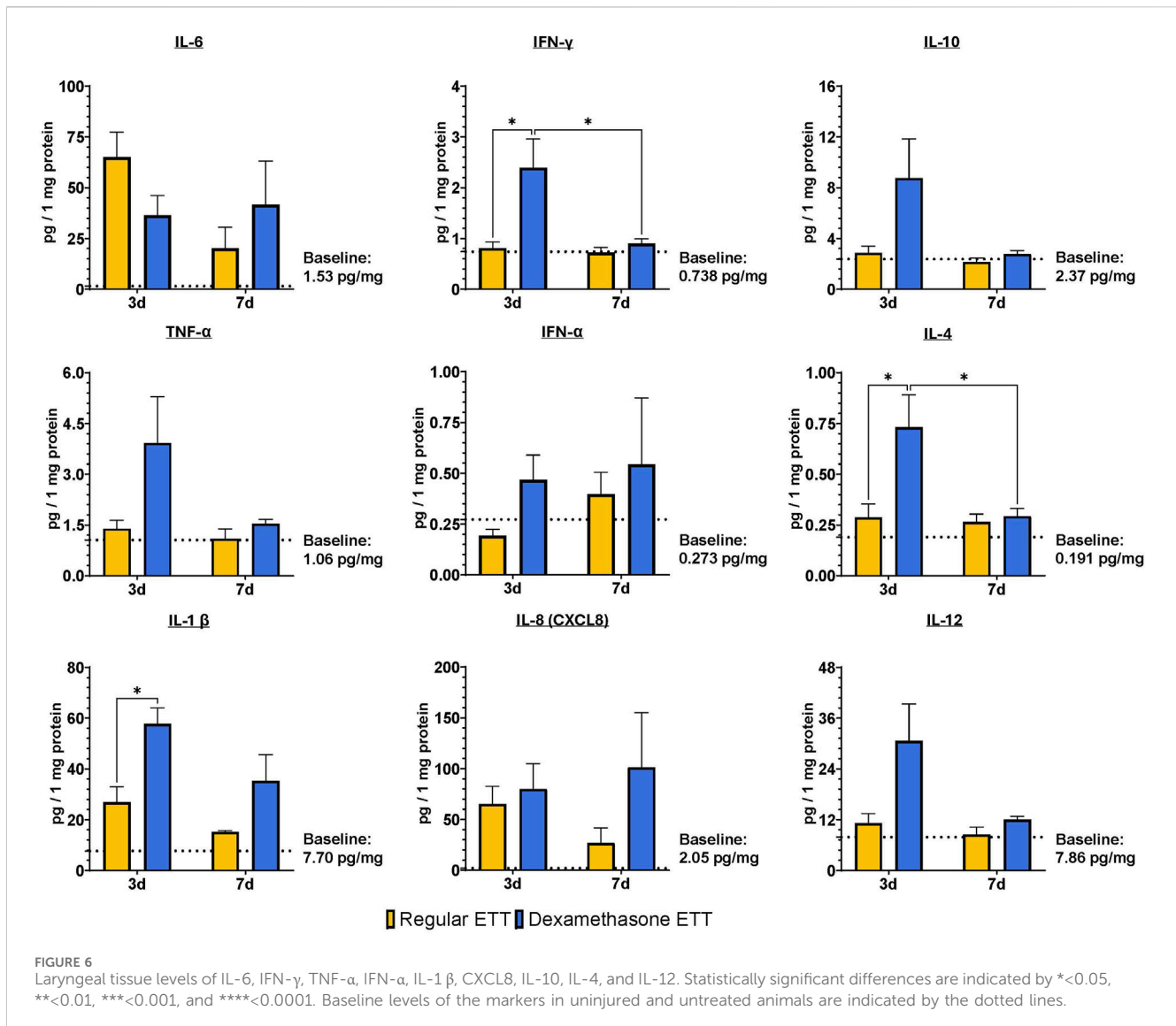


1994; Chen et al., 2014). Investigating the outcomes and interactions between inflammation and the microbiome in this context is essential for gaining a comprehensive understanding of the injury and providing insight into the mechanisms of laryngotracheal damage and healing. In the present study, we studied the effects of thermal injury and ETT placement on airway inflammation and microbial composition. Our approach involved the use of a drug-eluting endotracheal tube for localized delivery of dexamethasone, aiming to mitigate inflammation and prevent airway scarring.

Analysis of CT scans, particularly the surface area-to-volume (SA/V) ratios, can be a valuable metric in pathological studies for quantifying structural changes in the airway resulting from injury and noting onset or development of stenosis. Research has investigated SA/V in chronic obstructive pulmonary disease (COPD) and identified it as a potential imaging biomarker for airway remodeling, offering insight into both lung function decline and survival outcomes with disease (Bodduluri et al., 2021). The surface area-to-volume ratio significantly decreased following burn injury, as confirmed by 3D models generated from the large animal CT scans. These renderings visibly

demonstrate airway narrowing, particularly where the airway conforms closely around the ETT segments placed. This reduction in the surface area-to-volume ratio reflects structural changes in the airway post-injury, likely due to swelling or other injury-related alterations affecting airway dimensions and validates the insult of burn damage induced in the current model, and establishment of airway deficit prior to ETT placement.

Studies have shown that there is an association between specific taxonomic features of airway microbiome constituents and inflammatory conditions. In cases of COPD and asthma, the phyla Firmicutes, Proteobacteria, Actinobacteria, and Bacteroidetes have been identified as predominant (Ramsheh et al., 2021; Wang et al., 2016; Leiten et al., 2020; Millares et al., 2015; Pragman et al., 2012; Tangedal et al., 2019; Marri et al., 2013; Morimoto et al., 2024). While these phyla are also dominant in a healthy human airway (Santacroce et al., 2020; Elgamil et al., 2021; Valverde-Molina and García-Marcos, 2023; Haldar et al., 2020), changes in their relative abundance, especially at the genera level, differ significantly between various respiratory conditions. Notably, *Prevotella*, *Streptococcus*, *Haemophilus*, and *Moraxella* are consistently

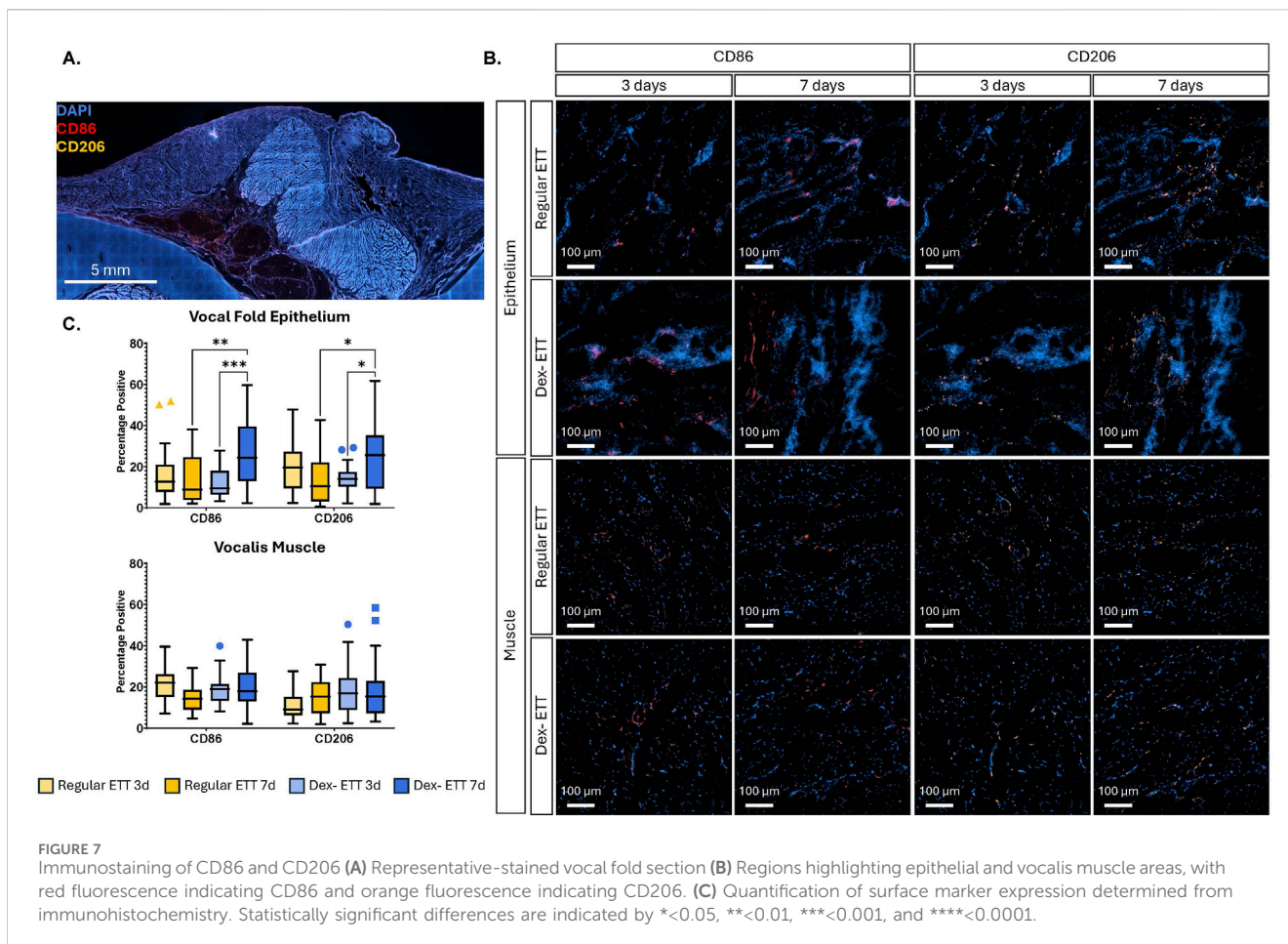


prevalent when comparing differences between COPD patients and healthy controls (Ramsheh et al., 2021; Wang et al., 2016; Wang et al., 2019). These shifts in microbial composition are often driven by host inflammatory milieu and *vice versa*, making anti-inflammatory interventions particularly relevant in managing such conditions. Dexamethasone, primarily recognized for its anti-inflammatory and immunosuppressive properties, is typically used to maintain airway patency while patients are also given prophylactic antibiotics to control infection and target bacterial pathogens. Some studies have indicated that dexamethasone may reduce the efficacy of certain antibiotics, such as those targeting *Staphylococcus aureus* and *Pseudomonas aeruginosa* (Rodrigues et al., 2017). However, the combined use of corticosteroids and antimicrobial drugs has also proven to improve the effectiveness of treatment in other cases (Neher et al., 2008; Chellappan et al., 2022). While the impact of dexamethasone on changes in the microbiome and the impact of the evolving microbiome on local inflammation is anticipated, there is limited literature to identify causal relationships or specific therapeutic regimen to simultaneously

target both the inflammation and potential microbial pathogenesis.

While many studies have investigated the presence of unique taxa in inflammatory airway diseases, there is a notable gap in characterizing the microbiome of the burn injured airway. An investigation of the airway microbiota after inhalation injury in burn patients revealed a significant enrichment of *Prevotella melaninogenica* and *Staphylococcus* within 3 days of injury (Walsh et al., 2017). While our study could not detect bacterial changes at the species level, we observed significant positive log fold changes for *Prevotella_7* and negative log fold changes for *Staphylococcus* at 3 days post-burn injury and ETT placement. While these changes were no longer significant after 7 days, it suggests early transient shifts in the airway microbiota with peak acute inflammation, with specific bacterial populations fluctuating in response to the initial injury and intervention.

We also observed increased log fold changes in *Bergeriella*, *Bacteroides*, and *Peptostreptococcus* at 3 days, with even more pronounced changes at 7 days in the burn injured airway. Some bacteria typically associated with the oral and gut microbiota can be

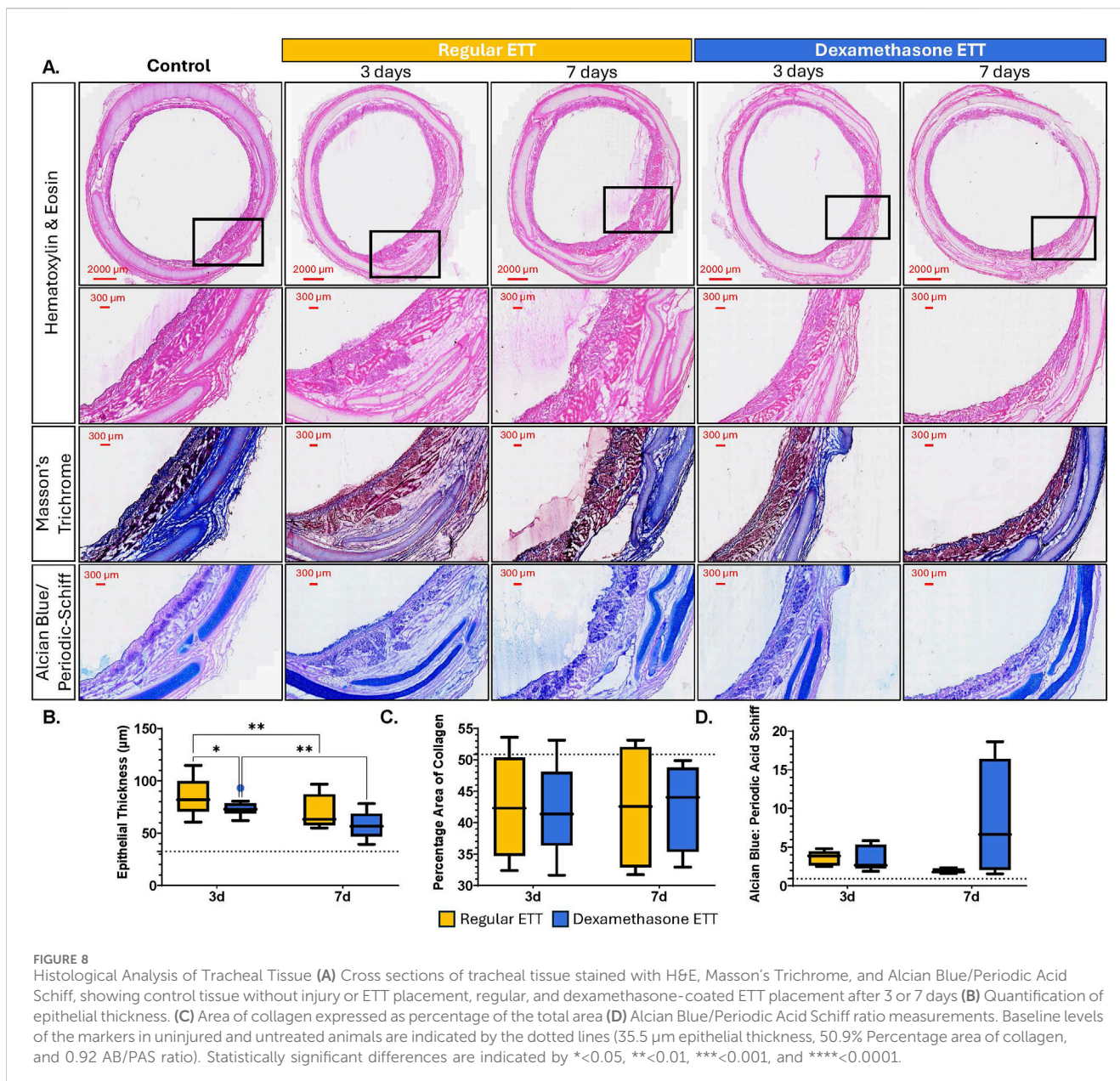


found in other body sites, such as the respiratory tract, in cases of dysbiosis, when mucosal barriers are compromised, or accidental inhalation of oropharyngeal or gastric contents known clinically as aspiration (Marik, 2001; Imai et al., 2021; Özçam and Lynch, 2024). *Bacteroides* and *Peptostreptococcus* are both anaerobic bacteria that have previously been implicated in the pathogenesis of aspiration pneumonia (Finegold, 1995; DiBardino and Wunderink, 2015; Lode, 1988). In particular, species of *Peptostreptococcus* have been shown to increase pro-inflammatory cytokine production, such as IL-1 β , in macrophages (Tanabe et al., 2007). *Bacteroides* species, typically related to the gut microbiome, have been linked to immunomodulatory polysaccharides that induce anti-inflammatory cytokines such as IL-10 which help control innate inflammatory responses under certain conditions (Ramakrishna et al., 2019; Chang et al., 2017; Mazmanian et al., 2008). While *Bergeriella* is less commonly reported, its presence in this study could indicate dysbiosis or an opportunistic infection, given its increase alongside *Bacteroides* and *Peptostreptococcus*. These microbes may favor the altered conditions present in the burn injured airway environment, potentially thriving with the presence of an ETT surface to adhere to.

Several studies have investigated the relationship between bacterial composition and the expression of inflammatory markers, revealing significant interactions between specific microbiota groups and human biomarkers of inflammation. For example, an abundance of *Moraxella* has been associated with the

expression of IL-17 and TNF inflammatory pathway in patients with COPD treated with inhaled corticosteroids, while IL-8 expression has been negatively correlated with bacteria in the genera *Haemophilus*, *Moraxella*, and *Streptococcus* (Ramsheh et al., 2021; Wang et al., 2016). Although no significant differences in abundance were found for *Haemophilus* and *Moraxella*, we noted a negative log fold change in *Streptococcus* at 7 days. Additionally, IL-8 expression at 7 days was elevated in the dexamethasone-coated ETT groups compared to regular ETTs. These findings suggest similar trends to those observed in COPD studies involving corticosteroid treatment, however, further studies are needed to determine statistical causality and to explore trends correlating other bacterial strains across cytokine/chemokine secretion profiles.

In the context of burn injury, increased levels of IL-6 and IL-10 and decreased levels of IL-7 in serum samples of pediatric patients with inhalation injury have been associated with fatal outcomes (Gauglitz et al., 2008). Investigation in older populations have demonstrated that the severity of inhalation injury induces systemically measurable effects on the concentrations of IL-1RA, IL-4, IL-6, IL-7, and IL-8 in plasma. Notably, higher levels of IL-1RA and IL-6, and lower levels of IL-4 and IL-7 were observed in deceased patients compared to survivors (Davis et al., 2013). In the present study, we also observed significant shifts in the airway microbiota and corresponding changes in cytokine levels following burn injury and ETT placement. Tissues treated with dexamethasone ETTs exhibited elevated



concentrations of cytokines compared to those with regular ETT placement and healthy controls. While inflammatory cytokines IL-6, IFN- α , and IL-8 increased from 3 to 7 days in the dexamethasone ETT groups, the levels of other cytokines decreased over the same period. This outcome may be contributed to an initial spike in cytokine levels at peak inflammation (3 days post-injury) due to the burn injury and the fiber-coated surface of the dexamethasone ETT, which potentially increases the inflammatory response and causes abrasion. Over time, as the dexamethasone exerts its anti-inflammatory effects, this initial inflammatory response subsides.

The immune cells in the upper airway following injury have been broadly identified including macrophages as one of the cell populations residing in the lamina propria (Catten et al., 1998; Boseley and Hartnick, 2006; Kaba et al., 2019). Polarized M1 macrophages are typically induced by pro-inflammatory

cytokines such as IFN- γ and IL-6, however, they can also be stimulated by bacterial lipopolysaccharides (Shapouri-Moghaddam et al., 2018; Lendeckel et al., 2022; Chen et al., 2023; Pérez and Rius-Pérez, 2022). These macrophages produce higher levels of pro-inflammatory cytokines, including IL-6, IL-1 β , TNF- α , and IL-12. In contrast, M2 macrophages are generally associated with anti-inflammatory responses producing cytokines like IL-4 and IL-10, and expressing TGF- β , which plays a key role in driving fibrosis in inflammatory conditions (Cheng et al., 2021; Ojiaku et al., 2017). However, the distinction between pro-inflammatory M1 macrophages and anti-inflammatory M2 macrophages can be an oversimplification, given the plasticity of macrophages in response to microenvironmental stimuli such as biofilm and ETT placement (Strizova et al., 2023). In our study, the significant increase in both CD86 and CD206 markers in the vocal fold epithelium in dexamethasone groups over time and compared to

regular ETT groups at 7 days likely reflects the increased biofilm formation observed on the coated ETTs. This conclusion is supported by the inclusions observed in 3D composites constructed from the μ CT and SEM which showed extensive bacterial adhesion on the surface, indicating interplay between biofilm formation and macrophage response.

We further investigated the structural changes in the trachea to better understand the tissue remodeling and healing process post burn-injury and ETT placement. Epithelial thickness measurements indicated an increase in the trachea epithelium after burn injury and ETT placement compared to control tissue, likely corresponding to epithelial hyperplasia. The significant reduction in tracheal epithelial thickness in both ETT types from 3 to 7 days aligns with the expected healing process, as the tissue gradually returns to its native state. Our group has previously explored epithelial ulceration, inflammation, and fibrosis in laryngeal tissue following inhalational burn injury and found minimal changes in degree of fibrosis and ulceration from 3 to 7 days, with both regular and dexamethasone ETTs, though inflammation scores were higher in the dexamethasone-coated ETTs compared to regular ETTs (Malka et al., 2023). Regarding the remodeling phase of collagen, there were no significant differences observed in the percentage area of collagen between the different ETT types. ETT groups showed a reduced collagen percentage compared to the healthy control. While an increase in collagen deposition is expected as part of the tissue's normal wound healing process, the time frame of the study may not have been sufficient for collagen accumulation. It is also possible that the increased epithelial thickening serves as a compensatory mechanism to protect against a weakened collagen matrix that is affected by injury and ETT placement.

The airway surfaces are lined with a protective layer of mucus that is continuously renewed to aid in the clearance of foreign pathogens and maintain respiratory health (Song et al., 2020; Pangani et al., 2023). However, in conditions such as inhalation injury or with the placement of an ETT, the production of these mucins can be disrupted leading to an imbalance in mucus composition that impairs the mucociliary clearance and increases the risk of infection (Powell et al., 2018; Cox et al., 2008; Cox et al., 2003; Koeppen et al., 2013). Our study observed the AB/PAS ratio to have increased levels of acidic mucins in tracheal tissue with ETT placement compared to control tissue. The subsequent reduction in the AB/PAS ratio over time suggests a shift towards a more stabilized mucosal environment as the initial inflammatory response subsides. Interestingly, the increased ratio observed in the dexamethasone ETT groups implies the use of the anti-inflammatory fiber coating is resulting in the production of more mucins, likely as the airway attempts to protect itself and facilitate the removal of the irritant. There has also been evidence that the inclusion of lubricating coatings on endotracheal tubes can lead to the further retention of epithelial mucosa and its secretory function (Miar et al., 2024).

There are several limitations to our study that merit consideration. The duration of the study was insufficient to fully capture the long-term effects of burn injury and ETT placement on airway healing and microbial composition changes. Although our injury model is validated across studies, variations in burn severity and the small sample size may have influenced the study outcomes

and limited our ability to identify statistically significant correlations between microbial shifts and cytokine levels. Additionally, findings from animal studies may not directly translate to human patients given the profound differences in the native microbiome. Further research is necessary to understand the implications of these findings in clinical settings.

Conclusion

This study reveals that burn injury and ETT placement significantly impact airway inflammation, structure, and microbiome. While both regular and dexamethasone-eluting ETTs affect the laryngotracheal environment, dexamethasone ETTs increased biofilm inclusions, certain inflammatory cytokines, and mucin production, possibly due to initial irritation from the ETT electrospun fiber coating. Additionally, there were notable shifts in the microbial community with burn injury, ETT type, and duration of placement, with significant differences in specific taxa observed at various time points. Future studies will focus on optimizing our drug-delivery technologies and strategies for managing burn-injured patients.

Data availability statement

All data generated during and/or analyzed during the current study are available in Supplementary Information file #2. Sequencing data is available in a publicly accessible repository. This data can be found here: <https://www.ncbi.nlm.nih.gov/BioProject/PRJNA1226158>. Further inquiries can be directed to the corresponding author.

Ethics statement

The animal study was approved by U.S. Air Force 59th Medical Wing Institutional Animal Care and Use Committee (protocol FWH20210102AR). The study was conducted in accordance with the local legislation and institutional requirements.

Author contributions

GG: Writing–review and editing, Data curation, Investigation, Writing–original draft. RM: Writing–review and editing, Methodology. RB: Writing–review and editing, Funding acquisition, Resources. GD: Writing–review and editing, Conceptualization, Methodology. TG: Conceptualization, Writing–review and editing, Project administration, Supervision.

Funding

The author(s) declare that financial support was received for the research, authorship, and/or publication of this article. Funding for this project was provided in part by the United States Army Institute of Surgical Research and

supported in part by the University of Texas at San Antonio, Office of Research (T2 Grant) and the Jacobson and Lutcher Brown Endowments.

Acknowledgments

The authors acknowledge the Kleberg Advanced Microscopy Center, Genomics Core, and Cell Analysis Core Facility at the University of Texas at San Antonio for support during this work.

Conflict of interest

The authors declare that the research was conducted in the absence of any commercial or financial relationships that could be construed as a potential conflict of interest.

Generative AI statement

The author(s) declare that no Generative AI was used in the creation of this manuscript.

References

- Aghasafari, P., George, U., and Pidaparti, R. (2019). A review of inflammatory mechanism in airway diseases. *Inflamm. Res.* 68, 59–74. doi:10.1007/s00011-018-1191-2
- Bittner, E., and Sheridan, R. (2023). Acute respiratory distress syndrome, mechanical ventilation, and inhalation injury in burn patients. *Surg. Clin. North Am.* 103, 439–451. doi:10.1016/j.suc.2023.01.006
- Bodduluri, S., Kizhakke Puliyakote, A., Nakhmani, A., Charbonnier, J. P., Reinhardt, J. M., and Bhatt, S. P. (2021). Computed tomography-based airway surface area-to-volume ratio for phenotyping airway remodeling in chronic obstructive pulmonary disease. *Am. J. Respir. Crit. Care Med.* 203, 185–191. doi:10.1164/rccm.202004-0951oc
- Boseley, M. E., and Hartnick, C. J. (2006). Development of the human true vocal fold: depth of cell layers and quantifying cell types within the lamina propria. *Ann. Otol. Rhinol. Laryngol.* 115, 784–788. doi:10.1177/000348940611501012
- Callahan, B. J., Sankaran, K., Fukuyama, J. A., McMurdie, P. J., and Holmes, S. P. (2016). Bioconductor workflow for microbiome data analysis: from raw reads to community analyses. *F1000Res* 5, 1492. doi:10.12688/f1000research.8986.2
- Carlisle, P., Marrs, J., Gaviria, L., Silliman, D. T., Decker, J. F., Brown Baer, P., et al. (2019). Quantifying vascular changes surrounding bone regeneration in a porcine mandibular defect using computed tomography. *Tissue Eng. Part C Methods* 25, 721–731. doi:10.1089/ten.tec.2019.0205
- Catten, M., Gray, S. D., Hammond, T. H., Zhou, R., and Hammond, E. (1998). Analysis of cellular location and concentration in vocal fold lamina propria. *Otolaryngol. Head. Neck Surg.* 118, 663–667. doi:10.1177/019459989811800516
- Chang, Y. C., Ching, Y. H., Chiu, C. C., Liu, J. Y., Hung, S. W., Huang, W. C., et al. (2017). TLR2 and interleukin-10 are involved in *Bacteroides fragilis*-mediated prevention of DSS-induced colitis in gnotobiotic mice. *PLoS One* 12, e0180025. doi:10.1371/journal.pone.0180025
- Chang-Hoon, L., and Eun Young, C. (2018). Macrophages and inflammation. *J. Rheum. Dis.* 25, 11–18. doi:10.4078/jrd.2018.25.1.11
- Charles, W. N., Collins, D., Mandalia, S., Matwala, K., Dutt, A., Tatlock, J., et al. (2022). Impact of inhalation injury on outcomes in critically ill burns patients: 12-year experience at a regional burns centre. *Burns* 48, 1386–1395. doi:10.1016/j.burns.2021.11.018
- Chellappan, D. K., Prasher, P., Shukla, S. D., Yee, T. W., Kah, T. K., Xyan, T. W., et al. (2022). Exploring the role of antibiotics and steroids in managing respiratory diseases. *J. Biochem. Mol. Toxicol.* 36, e23174. doi:10.1002/jbt.23174
- Chen, M.-C., Chen, M.-H., Wen, B.-S., Lee, M.-H., and Ma, H. (2014). The impact of inhalation injury in patients with small and moderate burns. *Burns* 40, 1481–1486. doi:10.1016/j.burns.2014.06.016
- Chen, S., Saeed, AFUH, Liu, Q., Jiang, Q., Xu, H., Xiao, G. G., et al. (2023). Macrophages in immunoregulation and therapeutics. *Signal Transduct. Target. Ther.* 8, 207. doi:10.1038/s41392-023-01452-1
- Cheng, P., Li, S., and Chen, H. (2021). Macrophages in lung injury, repair, and fibrosis. *Cells* 10, 436. doi:10.3390/cells10020436
- Cochran, A. (2009). Inhalation injury and endotracheal intubation. *J. Burn Care and Res.* 30, 190–191. doi:10.1097/bcr.0b013e3181923eb4
- Cox, R. A., Burke, A. S., Soejima, K., Murakami, K., Katahira, J., Traber, L. D., et al. (2003). Airway obstruction in sheep with burn and smoke inhalation injuries. *Am. J. Respir. Cell Mol. Biol.* 29, 295–302. doi:10.1165/rcmb.4860
- Cox, R. A., Mlcak, R. P., Chinkes, D. L., Jacob, S., Enkhbaatar, P., Jaso, J., et al. (2008). Upper airway mucus deposition in lung tissue of burn trauma victims. *Shock* 29, 356–361. doi:10.1097/shk.0b013e31814541dd
- Davis, C. S., Janus, S. E., Mosier, M. J., Carter, S. R., Gibbs, J. T., Ramirez, L., et al. (2013). Inhalation injury severity and systemic immune perturbations in burned adults. *Ann. Surg.* 257, 1137–1146. doi:10.1097/sla.0b013e318275f424
- DiBardino, D. M., and Wunderink, R. G. (2015). Aspiration pneumonia: a review of modern trends. *J. Crit. Care* 30, 40–48. doi:10.1016/j.jcrc.2014.07.011
- Domingue, J. C., Drewes, J. L., Merlo, C. A., Housseau, F., and Sears, C. L. (2020). Host responses to mucosal biofilms in the lung and gut. *Mucosal Immunol.* 13, 413–422. doi:10.1038/s41385-020-0270-1
- Dyamenahalli, K., Garg, G., Shupp, J. W., Kuprys, P. V., Choudhry, M. A., and Kovacs, E. J. (2019). Inhalation injury: unmet clinical needs and future research. *J. Burn Care and Res.* 40, 570–584. doi:10.1093/jbcr/irz055
- Edelman, D. A., Khan, N., Kempf, K., and White, M. T. (2007). Pneumonia after inhalation injury. *J. Burn Care Res.* 28, 241–246. doi:10.1097/bcr.0b013e318031d049
- Elgamal, Z., Singh, P., and Geraghty, P. (2021). The upper airway microbiota, environmental exposures, inflammation, and disease. *Med. Kaunas.* 57, 823. doi:10.3390/medicina57080823
- Fahy, J. V., and Dickey, B. F. (2010). Airway mucus function and dysfunction. *N. Engl. J. Med.* 363, 2233–2247. doi:10.1056/nejmra0910061
- Finogold, S. M. (1995). *Aspiration pneumonia Seminars in respiratory and critical care medicine: copyright© 1995 by. Thieme Medical Publishers, Inc., 475–483.*
- Foncerrada, G., Culnan, D. M., Capek, K. D., González-Trejo, S., Cambiaso-Daniel, J., Woodson, L. C., et al. (2018). Inhalation injury in the burned patient. *Ann. Plast. Surg.* 80, S98–S105. doi:10.1097/sap.0000000000001377
- Gaissert, H. A., Lofgren, R. H., and Grillo, H. C. (1993). Upper airway compromise after inhalation injury. Complex strictures of the larynx and trachea and their management. *Ann. Surg.* 218, 672–678. doi:10.1097/0000658-199311000-00014

Publisher's note

All claims expressed in this article are solely those of the authors and do not necessarily represent those of their affiliated organizations, or those of the publisher, the editors and the reviewers. Any product that may be evaluated in this article, or claim that may be made by its manufacturer, is not guaranteed or endorsed by the publisher.

Author disclaimer

The view(s) expressed herein are those of the author(s) and do not reflect the official policy or position of Brooke Army Medical Center, the U.S. Army Medical Department, the U.S. Army Office of the Surgeon General, the Department of the Army, the Department of the Air Force and Department of Defense or the U.S. Government.

Supplementary material

The Supplementary Material for this article can be found online at: <https://www.frontiersin.org/articles/10.3389/fbioe.2025.1524013/full#supplementary-material>

- Gauglitz, G. G., Finnerty, C. C., Herndon, D. N., Mlcak, R. P., and Jeschke, M. G. (2008). Are serum cytokines early predictors for the outcome of burn patients with inhalation injuries who do not survive? *Crit. Care* 12, R81. doi:10.1186/cc6932
- Gonzales, G., Malka, R., Marinelli, L., Lee, C. M., Miar, S., Cook, S., et al. (2024). Endotracheal tubes with dexamethasone eluting electrospun coating improve tissue mechanical function after upper airway injury. *Sci. Rep.* 14, 2821. doi:10.1038/s41598-024-53328-1
- Haldar, K., George, L., Wang, Z., Mistry, V., Ramsheh, M. Y., Free, R. C., et al. (2020). The sputum microbiome is distinct between COPD and health, independent of smoking history. *Respir. Res.* 21, 183. doi:10.1186/s12931-020-01448-3
- Hall-Stoodley, L., and McCoy, K. S. (2022). Biofilm aggregates and the host airway-microbial interface. *Front. Cell Infect. Microbiol.* 12, 969326. doi:10.3389/fcimb.2022.969326
- Huber-Lang, M., Lambris, J. D., and Ward, P. A. (2018). Innate immune responses to trauma. *Nat. Immunol.* 19, 327–341. doi:10.1038/s41590-018-0064-8
- Imai, K., Iinuma, T., and Sato, S. (2021). Relationship between the oral cavity and respiratory diseases: aspiration of oral bacteria possibly contributes to the progression of lower airway inflammation. *Jpn. Dent. Sci. Rev.* 57, 224–230. doi:10.1016/j.jdsr.2021.10.003
- Jones, S. W., Williams, F. N., Cairns, B. A., and Cartotto, R. (2017). Inhalation injury: pathophysiology, diagnosis, and treatment. *Clin. Plast. Surg.* 44, 505–511. doi:10.1016/j.cps.2017.02.009
- Kaba, S., Nakamura, R., Yamashita, M., Katsuno, T., Suzuki, R., Tateya, I., et al. (2019). Alterations in macrophage polarization in injured murine vocal folds. *Laryngoscope* 129 (4), E135–E142. doi:10.1002/lary.27523
- Koeppen, M., McNamee, E. N., Brodsky, K. S., Aherne, C. M., Faigle, M., Downey, G. P., et al. (2013). Detrimental role of the airway mucin Muc5ac during ventilator-induced lung injury. *Mucosal Immunol.* 6, 762–775. doi:10.1038/mi.2012.114
- Koh, T. J., and DiPietro, L. A. (2011). Inflammation and wound healing: the role of the macrophage. *Expert Rev. Mol. Med.* 13, e23. doi:10.1017/s1462399411001943
- Landini, G., Martinelli, G., and Piccinini, F. (2021). Colour deconvolution: stain unmixing in histological imaging. *Bioinformatics* 37, 1485–1487. doi:10.1093/bioinformatics/btaa847
- Leiten, E. O., Nielsen, R., Wiker, H. G., Bakke, P. S., Martinsen, E. M. H., Drengenes, C., et al. (2020). The airway microbiota and exacerbations of COPD. *ERJ Open Res.* 6, 00168–02020. doi:10.1183/23120541.00168-2020
- Lendeckel, U., Venz, S., and Wolke, C. (2022). Macrophages: shapes and functions. *ChemTexts* 8, 12. doi:10.1007/s40828-022-00163-4
- Lin, H., Eggesbo, M., and Peddada, S. D. (2022). Linear and nonlinear correlation estimators unveil undescribed taxa interactions in microbiome data. *Nat. Commun.* 13, 4946. doi:10.1038/s41467-022-32243-x
- Lin, H., and Peddada, S. D. (2020). Analysis of compositions of microbiomes with bias correction. *Nat. Commun.* 11, 3514. doi:10.1038/s41467-020-17041-7
- Lode, H. (1988). Microbiological and clinical aspects of aspiration pneumonia. *J. Antimicrob. Chemother.* 21 (Suppl. C), 83–87. doi:10.1093/jac/21.suppl_c.83
- Malka, R., Gonzales, G., Detar, W., Marinelli, L., Lee, C. M., Isaac, A., et al. (2023). Effect of continuous local dexamethasone on tissue biomechanics and histology after inhalational burn in a preclinical model. *Laryngoscope Investig. Otolaryngol.* 8, 939–945. doi:10.1002/liv.1093
- Marik, P. E. (2001). Aspiration pneumonitis and aspiration pneumonia. *N. Engl. J. Med.* 344, 665–671. doi:10.1056/nejm200103013440908
- Marri, P. R., Stern, D. A., Wright, A. L., Billheimer, D., and Martinez, F. D. (2013). Asthma-associated differences in microbial composition of induced sputum. *J. Allergy Clin. Immunol.* 131, 346–352.e3. doi:10.1016/j.jaci.2012.11.013
- Martin, M. (2011). *Cutadapt removes adapter sequences from high-throughput sequencing reads*, 17, 3.
- Mazmanian, S. K., Round, J. L., and Kasper, D. L. (2008). A microbial symbiosis factor prevents intestinal inflammatory disease. *Nature* 453, 620–625. doi:10.1038/nature07008
- McMurdie, P. J., and Holmes, S. (2013). phyloseq: an R package for reproducible interactive analysis and graphics of microbiome census data. *PLoS One* 8, e61217. doi:10.1371/journal.pone.0061217
- Miar, S., Gonzales, G., Dion, G., Ong, J. L., Malka, R., Bizios, R., et al. (2024). Electrospun composite-coated endotracheal tubes with controlled siRNA and drug delivery to lubricate and minimize upper airway injury. *Biomaterials* 309, 122602. doi:10.1016/j.biomaterials.2024.122602
- Millares, L., Perez-Brocal, V., Ferrari, R., Gallego, M., Pomares, X., García-Núñez, M., et al. (2015). Functional metagenomics of the bronchial microbiome in COPD. *PLoS One* 10, e0144448. doi:10.1371/journal.pone.0144448
- Mishra, S. K., Baidya, S., Bhattarai, A., Shrestha, S., Homagain, S., Rayamajhee, B., et al. (2024). Bacteriology of endotracheal tube biofilms and antibiotic resistance: a systematic review. *J. Hosp. Infect.* 147, 146–157. doi:10.1016/j.jhin.2024.03.004
- Monteiro, D., Silva, I., Egipito, P., Magalhães, A., Filipe, R., Silva, A., et al. (2017). Inhalation injury in a burn unit: a retrospective review of prognostic factors. *Ann. Burns Fire Disasters* 30, 121–125.
- Morimoto, C., Matsumoto, H., Nomura, N., Sunadome, H., Nagasaki, T., Sato, S., et al. (2024). Sputum microbiota and inflammatory subtypes in asthma, COPD, and its overlap. *J. Allergy Clin. Immunol. Glob.* 3, 100194. doi:10.1016/j.jacig.2023.100194
- Moser, C., Pedersen, H. T., Lerche, C. J., Kolpen, M., Line, L., Thomsen, K., et al. (2017). Biofilms and host response – helpful or harmful. *APMIS* 125 (4), 320–338. doi:10.1111/apm.12674
- Natalini, J. G., Singh, S., and Segal, L. N. (2023). The dynamic lung microbiome in health and disease. *Nat. Rev. Microbiol.* 21, 222–235. doi:10.1038/s41579-022-00821-x
- Neher, A., Armitz, R., Gstottner, M., Schafer, D., Kross, E. M., and Nagl, M. (2008). Antimicrobial activity of dexamethasone and its combination with N-chlorotaurine. *Arch. Otolaryngol. Head. Neck Surg.* 134, 615–620. doi:10.1001/archotol.134.6.615
- Ojiaku, C. A., Yoo, E. J., and Panettieri, R. A., Jr (2017). Transforming growth factor β 1 function in airway remodeling and hyperresponsiveness. The missing link? *Am. J. Respir. Cell Mol. Biol.* 56, 432–442. doi:10.1165/rcmb.2016-0307tr
- Orozco-Peláez, Y. A. (2018). Airway burn or inhalation injury: should all patients be intubated? *Colombian J. Anesthesiol.* 46, 26–31. doi:10.1097/cj9.000000000000042
- Özçam, M., and Lynch, S. V. (2024). The gut–airway microbiome axis in health and respiratory diseases. *Nat. Rev. Microbiol.* 22, 492–506. doi:10.1038/s41579-024-01048-8
- Pangeni, R., Meng, T., Poudel, S., Sharma, D., Hutsell, H., Ma, J., et al. (2023). Airway mucus in pulmonary diseases: muco-adhesive and muco-penetrating particles to overcome the airway mucus barriers. *Int. J. Pharm.* 634, 122661. doi:10.1016/j.ijpharm.2023.122661
- Pérez, S., and Rius-Pérez, S. (2022). Macrophage polarization and reprogramming in acute inflammation: a redox perspective. *Antioxidants (Basel)* 11, 1394. doi:10.3390/antiox11071394
- Powell, J., Garnett, J. P., Mather, M. W., Cooles, F. A. H., Nelson, A., Verdon, B., et al. (2018). Excess mucin impairs subglottic epithelial host defense in mechanically ventilated patients. *Am. J. Respir. Crit. Care Med.* 198, 340–349. doi:10.1164/rccm.201709-1819oc
- Pragman, A. A., Kim, H. B., Reilly, C. S., Wendt, C., and Isaacson, R. E. (2012). The lung microbiome in moderate and severe chronic obstructive pulmonary disease. *PLoS One* 7, e47305. doi:10.1371/journal.pone.0047305
- Quast, C., Pruesse, E., Yilmaz, P., Gerken, J., Schweer, T., Yarza, P., et al. (2013). The SILVA ribosomal RNA gene database project: improved data processing and web-based tools. *Nucleic Acids Res.* 41, D590–D596. doi:10.1093/nar/gks1219
- Ramakrishna, C., Kujawski, M., Chu, H., Li, L., Mazmanian, S. K., and Cantin, E. M. (2019). Bacteroides fragilis polysaccharide A induces IL-10 secreting B and T cells that prevent viral encephalitis. *Nat. Commun.* 10, 2153. doi:10.1038/s41467-019-09884-6
- Ramsheh, M. Y., Haldar, K., Esteve-Codina, A., Purser, L. F., Richardson, M., Muller-Quernheim, J., et al. (2021). Lung microbiome composition and bronchial epithelial gene expression in patients with COPD versus healthy individuals: a bacterial 16S rRNA gene sequencing and host transcriptomic analysis. *Lancet Microbe* 2 (7), e300–e310. doi:10.1016/s2666-5247(21)00035-5
- Rodrigues, A., Gomes, A., Marcal, P. H., and Dias-Souza, M. V. (2017). Dexamethasone abrogates the antimicrobial and antibiofilm activities of different drugs against clinical isolates of *Staphylococcus aureus* and *Pseudomonas aeruginosa*. *J. Adv. Res.* 8, 55–61. doi:10.1016/j.jare.2016.12.001
- Ronkar, N. C., Galet, C., Richey, K., Foster, K., and Wibbenmeyer, L. (2023). Predictors and impact of pneumonia on adverse outcomes in inhalation injury patients. *J. Burn Care and Res.* 44, 1289–1297. doi:10.1093/jbcr/irad099
- Santacroce, L., Charitos, I. A., Ballini, A., Inchingolo, F., Luperto, P., De Nitto, E., et al. (2020). The human respiratory system and its microbiome at a glimpse. *Biol. (Basel)* 9 (10), 318. doi:10.3390/biology9100318
- Shapouri-Moghaddam, A., Mohammadian, S., Vazini, H., Taghadosi, M., Esmaili, S., Mardani, F., et al. (2018). Macrophage plasticity, polarization, and function in health and disease. *J. Cell. Physiology* 233, 6425–6440. doi:10.1002/jcp.26429
- Smith, D. L., Cairns, B. A., Ramadan, F., Dalston, J. S., Fakhry, S. M., Rutledge, R., et al. (1994). Effect of inhalation injury, burn size, and age on mortality: a study of 1447 consecutive burn patients. *J. Trauma* 37, 655–659. doi:10.1097/00005373-199410000-00021
- Song, D., Cahn, D., and Duncan, G. A. (2020). Mucin biopolymers and their barrier function at airway surfaces. *Langmuir* 36, 12773–12783. doi:10.1021/acs.langmuir.0c02410
- Strizova, Z., Benesova, I., Bartolini, R., Novsedlak, R., Cecdlova, E., Foley, L., et al. (2023). M1/M2 macrophages and their overlaps - myth or reality? *Clin. Sci. (Lond)* 137, 1067–1093. doi:10.1042/cs20220531
- Tanabe, S., Bodet, C., and Grenier, D. (2007). Peptostreptococcus micros cell wall elicits a pro-inflammatory response in human macrophages. *J. Endotoxin Res.* 13, 219–226. doi:10.1177/0968051907081869

Tangedal, S., Nielsen, R., Aanerud, M., Persson, L. J., Wiker, H. G., Bakke, P. S., et al. (2019). Sputum microbiota and inflammation at stable state and during exacerbations in a cohort of chronic obstructive pulmonary disease (COPD) patients. *PLoS One* 14, e0222449. doi:10.1371/journal.pone.0222449

Torres, A., Lee, N., Cilloniz, C., Vila, J., and Van der Eerden, M. (2016). Laboratory diagnosis of pneumonia in the molecular age. *Eur. Respir. J.* 48, 1764–1778. doi:10.1183/13993003.01144-2016

Valverde-Molina, J., and García-Marcos, L. (2023). Microbiome and asthma: microbial dysbiosis and the origins, phenotypes, persistence, and severity of asthma. *Nutrients* 15, 486. doi:10.3390/nu15030486

Walsh, D. M., McCullough, S. D., Yourstone, S., Jones, S. W., Cairns, B. A., Jones, C. D., et al. (2017). Alterations in airway microbiota in patients with PaO₂/FiO₂ ratio \leq 300 after burn and inhalation injury. *PLoS One* 12, e0173848. doi:10.1371/journal.pone.0173848

Wang, Z., Bafadhel, M., Haldar, K., Spivak, A., Mayhew, D., Miller, B. E., et al. (2016). Lung microbiome dynamics in COPD exacerbations. *Eur. Respir. J.* 47, 1082–1092. doi:10.1183/13993003.01406-2015

Wang, Z., Maschera, B., Lea, S., Kolsum, U., Michalovich, D., Van Horn, S., et al. (2019). Airway host-microbiome interactions in chronic obstructive pulmonary disease. *Respir. Res.* 20, 113. doi:10.1186/s12931-019-1085-z